

Polymer capture, folds, and translocation in a solitary nanopore

Swarnadeep Seth and Aniket Bhattacharya*

¹*Department of Physics, University of Central Florida, Orlando, Florida 32816-2385, USA*

(Dated: November 23, 2021)

DNA capture with high fidelity is an essential part of nanopore translocation. We report several important aspects of the capture process and subsequent translocation of a model DNA polymer through a solid-state nanopore in presence of an extended electric field using the Brownian dynamics simulation that enables us to record statistics of the conformations at every stage of the translocation process. By releasing the equilibrated DNAs from different equipotentials, we observe that the capture time distribution depends on the initial starting point and follows a Poisson process. The field gradient elongates the DNA on its way towards the nanopore and favors a successful translocation even after multiple failed threading attempts. Even in the limit of an extremely narrow pore, a fully flexible chain has a finite probability of hairpin-loop capture while this probability decreases for a stiffer chain and promotes single file translocation. Our studies for the first time identify and differentiate characteristic distributions of the mean first passage time due to single file translocation from those due to translocation of different types of folds and provide direct evidences of the interpretation of the experimentally observed folds [M. Gershow *et al.*, Nat. Nanotech. **2**, 775 (2007) & M. Mihovilovic *et al.* Phys. Rev. Letts. **110**, 028102 (2013)] in solitary nanopores.

PACS numbers: 87.64.-t, 36.20.-r, 87.85.Qr

Electromechanical transport in solid-state nanopores and nanochannels has received substantial attention in recent years [1–6]. By applying a voltage bias across the nanochannel, the charged molecules can be electrophoretically transported along the axial direction of the channel with high speed, which may be exploited to characterize the molecular events. Among various approaches for nanopore sequencing [7–10], single file translocation [11, 12] has recently been demonstrated to achieve ultra-fast DNA sequencing at a high speed [13–15]. To realize both high-speed and high-accuracy sequencing, single file translocation through the nanopore in a field-aligned manner is strongly demanded and has been widely explored in recent years [16, 17].

The capture of a dsDNA in the context of nanopore translocation has been studied experimentally [18, 19] and using different theoretical [20–22] and simulation methods [23–26]. The DNA gets stretched by the electric field (E-field) gradient extended beyond the nanopore, in process of getting captured at the nanopore orifice and translocates through it. Here, the length of DNA is not a limiting factor for the single-file translocation process as once captured by the nanopore target, it is highly probable that translocation will take place. The major drawback of this method is the low capture probability that results from a competition between ionic concentration polarization, DNA conformation, and the thermal fluctuation. The increase of capture efficiency should be considered in any design of a nanopore device for DNA sequencing because a low capture probability may also lead to an increased error rate in sequencing statistics.

In this letter, we unveil the details of how a polymer

makes its way from the bulk solution towards a nanopore, gets trapped by a guiding electric field that extends beyond the pore, and completes the translocation process. The entire journey from capture to translocation can be broken down into three stages. Once the DNA polymer is released into the solution, it wanders diffusively until it encounters the electric field pull from the nanopore. In the later stages, polymer motion evolves to that of a drift-diffusion under the guiding electric field lines, and the capture occurs as it approaches the critical distance for the capture from the nanopore orifice [25, 26]. In general for a successful capture, the polymer has to overcome the entropic barrier [20] by restricting the conformational degrees of freedom for the chain, which often takes a significant amount of time and includes multiple failed attempts. This capture process is non-equilibrium in nature and is affected by a number of factors, including the chain length, the initial release point, the chain stiffness, and the electric field strength. Following the successful capture, translocation begins, and the tension front quickly draws the chain into the *trans* side [27]. The letter delineates succinctly how each of these factors contributes to the capture and translocation. Understanding these three stages from coarse-grained (CG) simulation enables readers to visualize the process in the nanometer length scale which will help to design better nanopore devices of improved accuracy.

• **Effect of the electric field in pre-translocation:** Our CG model of a dsDNA consists of 256 beads of diameter of σ , that mimics a $4\mu\text{m}$ long λ -phage DNA with 48 bp resolution associated with a single bead. The starting configuration of our studies is a 4-times-Rouse-relaxed chain having a few beads residing inside the nanopore those experience the localized electric field strictly inside the pore. At the start of the translocation process, the beads inside the nanopore experience a downward pulling

* Author to whom the correspondence should be addressed; Aniket.Bhattacharya@ucf.edu

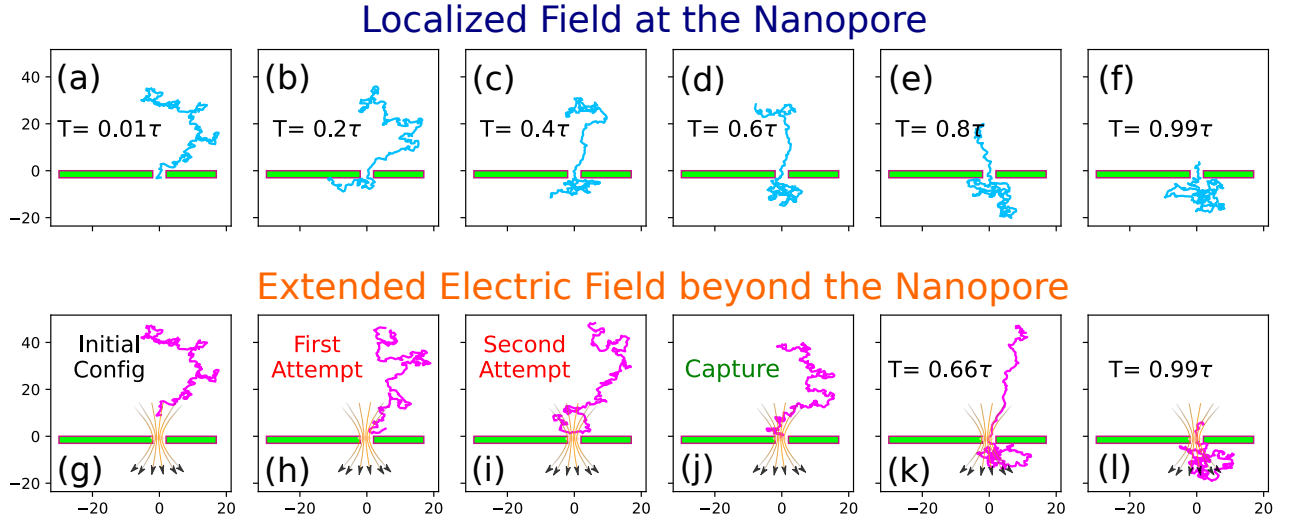


FIG. 1. A series of simulations snapshots (a)-(f) in progressive time show the translocation process of the polymer in presence of localized force bias applied in the nanopore thickness. τ is the total translocation time of the chain. (g)-(l) The same polymer configuration is released from the equipotential surface $d = 4.0$ away from the pore in presence of the electric field which extends beyond the nanopore. During the capture process, the polymer makes a few unsuccessful attempts shown in (h) and (j) before one end threads into the nanopore. (k)-(l) show the translocation of the captured polymer through the nanopore under the electric field gradient.

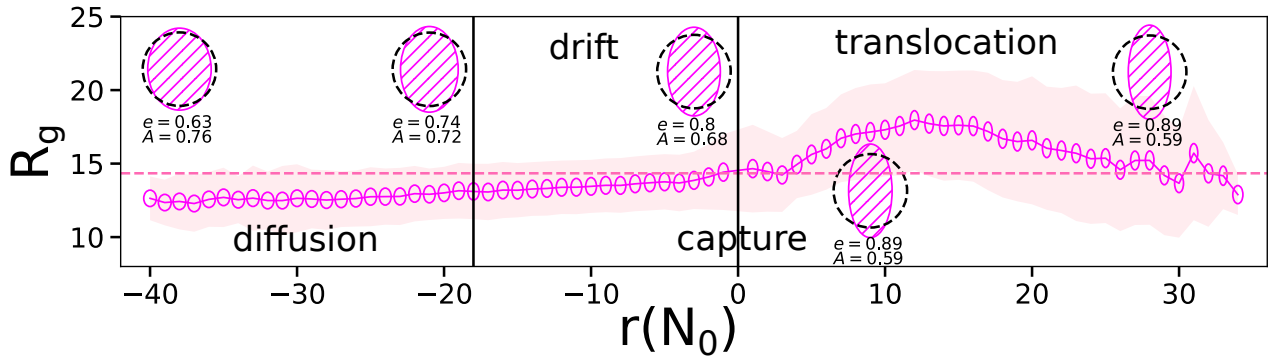


FIG. 2. Polymer radius of gyration as a function of first monomer distance $r(N_0)$ from the pore. The effective radius of gyration of the polymer at a distance is represented by an ellipse having the major/minor axis representing transverse/longitudinal component respectively. The average R_g is denoted by the magenta dotted line. R_g at different phases (a) diffusion dominated (b) drift dominated and capture (c) translocation and escape are presented in the inset ellipses and compared against a unit circle in black. e and A denote the eccentricity and the area of the ellipses respectively. The drift region is identified from the diffusion dominated region by marking the inflection point of the R_g .

force while the tension front [27] propagates through the chain backbone in the opposite direction of translocation that first uncoils the chain. The chain is quickly sucked into the pore when the tension front hits the last bead [28]. This entire process is demonstrated in Fig. 1 ((a)-(f)).

Though decades of theoretical and numerical studies have been carried out starting with a polymer configuration captured at the nanopore [2, 5, 6], this process does not resemble an experiment situation where the polymer is first released into the solution and later captured

at the pore by applying a steep voltage bias across the pore. To understand this entire process from the capture to the translocation, we study the case where the electric field extends beyond a cylindrical nanopore in both the *cis* and the *trans* directions. We use the Finite Element method [29] to solve the Poisson equation to construct the electric field around a solitary nanopore having a diameter and thickness of 2σ . Unlike the case of a localized E-field, the polymer gets elongated in the extended E-field [23] due to the gradient of the electric field, which is strongest at and near the pore. The average radius of gyration $\langle R_g \rangle$ reflects the shape of a polymer and to char-

acterize this dynamic deformation process we compare the transverse and longitudinal radius of gyration as the polymer drifts towards the pore. We define the longitudinal and the transverse gyration radii as $\langle Rg_{\parallel} \rangle = \sqrt{\langle R_y^2 \rangle}$ and $\langle Rg_{\perp} \rangle = \sqrt{\langle Rg_x^2 \rangle + \langle Rg_z^2 \rangle}$, and construct a radius of gyration ellipse using $\langle Rg_{\parallel} \rangle / \langle Rg_{\perp} \rangle$ as major/minor axis respectively. Far away from the pore, the polymer remains almost unaffected by the electric field, resembling the equilibrium configuration with $\langle Rg_{\parallel} \rangle \simeq \langle Rg_{\perp} \rangle$. As polymer drifts along the field lines, $\langle Rg_{\parallel} \rangle$ extends over $\langle Rg_{\perp} \rangle$ enhancing the eccentricity of the gyration ellipse as shown in Fig. 2. The gyration ellipse eccentricity increases steadily until the polymer translocates through the nanopore completely as discussed below.

• **Polymer drift and capture at the nanopore:** The process of capture requires the polymer to overcome the potential barrier by adjusting its conformational entropy resembling Kramer’s escape problem [30, 31]. The capture is being a non-equilibrium process [32] where field strength dominates over the diffusion near the pore leading to a directed motion of either end of the polymer getting captured. We release the equilibrated DNA polymer from different positions located at the surface of the equipotential spheres of radius d (measured from the center of the nanopore) starting with a larger value of d . We use potential surfaces as the starting locations instead of fixed distances as this would be easier to mimic in the experiments and can be compared unambiguously. For

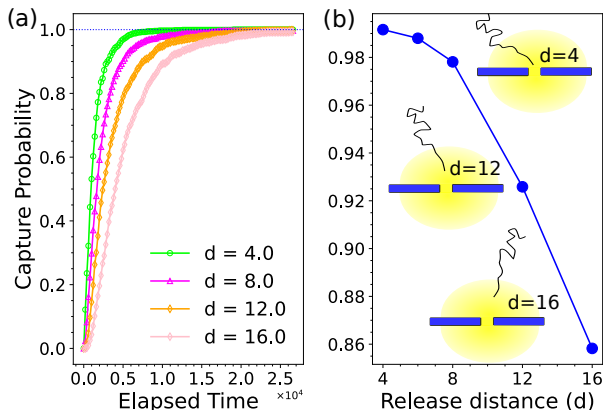


FIG. 3. (a) Probability of capture of a polymer in the nanopore orifice as the time progresses after the polymer is released from different equipotential distances $d = 4.0$ (\circ), 8.0 (\triangle), 12.0 (\diamond), and 16.0 (\diamond). (b) Dependence of the capture probability as the release distance d is varied from the pore orifice.

a fixed voltage bias, we demonstrate that the capture probability strongly depends on the initial release location of the polymer. After the release, we monitor the journey of the fully flexible polymers until translocation. The capture probability is a ratio of the number of polymers captured over the number at the beginning, shown in Fig 3 (a), and increases with time. The closer the

equipotential release surface from the pore, the quicker the capture takes place. By increasing the release distance, our study shows that there is a finite probability (shown in Fig. 3 (b)) that polymers drift away from the pore as the field strength becomes weaker for the distant equipotential surfaces. Though a polymer is captured its motion barely follows the curvature of a single field line going straight through the nanopore. A successful capture often requires multiple failed attempts but with an increasing number of failed attempts, the probability of capture also gets enhanced as the polymer gyration radius gets compressed by the E-field and remains in the vicinity of the nanopore opening. Fig. 4(a)-(d) we show the capture time distributions which sum up the polymer journey from release to capture including the failed attempts. With increasing d , the average capture time increases which suggests a longer wonder time when released from a weaker potential. The distribution closely resembles a “memoryless” Poisson process as the arrival of polymers at the pore mouth are independent events in time and follow the shape of an exponential distribution where mean and standard deviation are almost identical. It is worth mentioning that the Poissons distributions of Fig. 4((a)-(d)) produced by the BD simulation are the same as observed experimentally by Gershow and Golovchenko [18]

However, as first suggested by Mihovilovic *et al.* to explain their experimental results that during capture, a polymer can thread into the pore with three different conformations (Type 1, Type 2-1, Type 2) events [19] depending on the relative location of the chain with respect to the pore as shown in Fig. 4((i)-(t)). In Type 1 events one end of the polymer threads (Fig. 4(i,m,q)), in Type 2-1 a random location capture occurs, while the symmetric threadings are Type 2 events (Fig. 4(j,n,r) & (k,o,s)). Not only we observe these threading conformations in our simulation studies, in addition, our simulation provides the fraction of events belonging to these three categories as shown Fig. 4((e)-(h)) insets. For a closer release from $d = 4.0$, Type 1 capture percentage is marginally greater than Type 2-1 events but for all the other cases $d \geq 6.0$, Type 2-1 is the most abundant event. On the contrary, Type 2 events are rare occurrences ($\leq 2\%$) compared to the rest.

• **Translocation:** Recent theories [32] indicate that translocation depends on the polymer’s initial conformation and the degree of equilibration. In an experimental setup electric field gradient, flow of the charged ions, nanopore surface charge, and pH of the solution influence on the polymer shape during capture. We calculate the average end-to-end distance $\langle R_{end} \rangle$ of the polymer at the instance of capture to study its effect on the translocation time. During the pre-capture phase, a polymer undergoes stretching deformation due to the unidirectional field gradient and $\langle R_{end} \rangle$ deviates from the equilibrium end to end distance which is more prominent when starting from a distant equipotential from the pore mouth. The $\langle R_{end} \rangle$ histograms in Fig. 4((u)-(x)) become slightly right

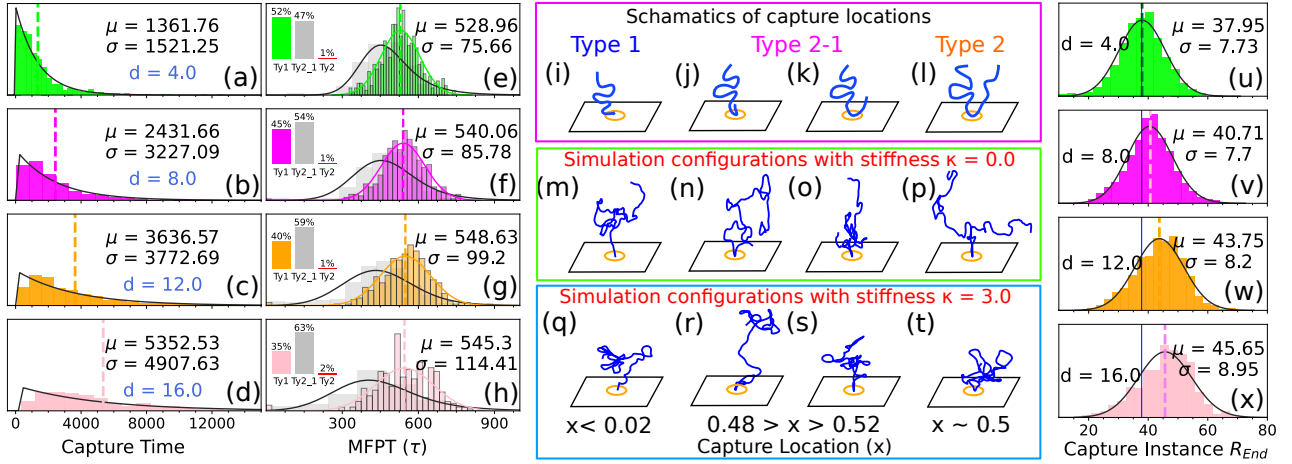


FIG. 4. Distribution of capture time after releasing a polymer from different equipotential distances (a) $d = 4.0$, (b) 6.0 , (c) 8.0 , and (d) 16.0 respectively. The black envelopes show the exponential fits of the distributions and the averages are marked by dashed lines. The mean first passage time histograms (e)-(h) follow Gaussian shape with average μ and standard deviation σ are obtained from single file translocation (Type 1) events for the same equipotential release distances. The Type 2-1 translocations are faster than Type 1 events and are shown in silver histograms which are also predominant occurrences for higher d . Type 2 events are relatively rare and the bar plots in the insets represent the occurrence of these three types of capture events in a percentage scale. (i)-(l) Rendition of the different ways a polymer thread through the nanopore and translocates. The capture location x denotes the normalized monomer index m/N which first threads into the nanopore; (i) The single file capture events where either of the ends gets captured are denoted as Type1 translocation. (j)-(k) show the Type2-1 events in which polymer is captured at any random location except at the ends and in the symmetric location. (l) Type2 events indicate the symmetrical capture cases. (m)-(p) and (q)-(t) denote the same using the actual coordinates from BD simulation for the stiffness parameters $\kappa = 0$ and $\kappa = 3.0$ respectively. End to end distance R_{end} distributions of a polymer at the moment of capture at the nanopore orifice after being released from four different equipotential distances $d = 4.0, 8.0, 12.0$, and 16.0 are shown in (u - x) subplots. The black envelopes denote the exponentially modified Gaussian fits of the distributions. Average and standard deviation of the distributions are marked in μ and σ respectively and corresponding $\langle R_{end} \rangle$ are shown in the colored dashed lines while the blue line represents the average end to end distances of the starting configurations.

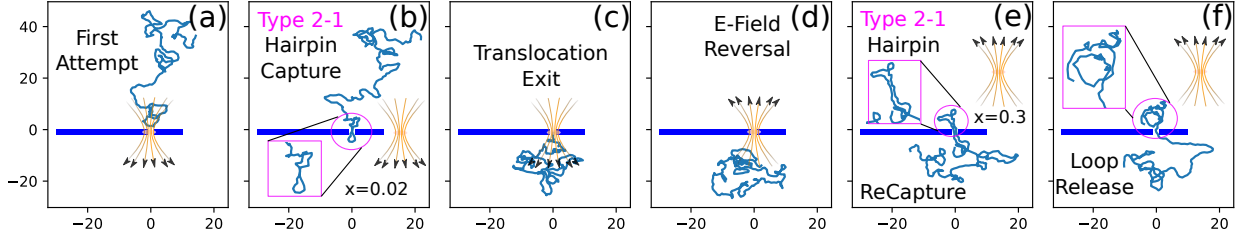


FIG. 5. The series of snapshots show the multi-capture process of a single polymer by altering the voltage bias. (a) The first attempt of threading from the cis side (b) hairpin capture (Type 2-1), and (c) translocation from cis side to the trans side. (d) After the reversal of the E-field (e) the same polymer gets captured from the bottom side of the pore. The hairpin loop structure is shown in the inset and at first both ends translocate at the same time. (f) Single end translocation begins after the unwinding of the loop.

skewed for higher d and $\langle R_{end} \rangle$ increases by 5–20 % from the equilibrium average. However, the mean first passage time (MFPT) distributions of 1000 independently captured polymers show a counter intuitive outcome, indicating a faster translocation time for higher d where we previously observed that $\langle R_{end} \rangle$ is large. This apparent contradiction is resolved when we filter out Type 2-1 events from Type 1 events and plot the translocation time histograms separately for each type of event as

shown in Fig. 4((e)-(h)). The translocation of Type 2-1 and Type 2 captured configurations are inherently different and faster than a single file translocation event as both ends of a hairpin loop configuration thread through the nanopore simultaneously until one end translocates completely and the loop unwinds. This phenomenon is explained in Fig. 5. For Type 1 translocation event, average MFPT and spread increase with d (shown in the colored histograms in Fig. 4((e)-(h))), while for the Type

2-1 events a faster MFPT is obtained (silver histograms).

- **Post-translocation compression:** Translocation being a faster process in presence of an electric field gradient, the polymer configuration gets compressed in the post translocation phase. Fig. 2 demonstrates the compression factor as the area of the gyration ellipse decreases more than 20% compared to its pre-translocation stage. After translocation, both the eccentricity and area of $\langle Rg \rangle$ ellipse remain constant but the fluctuation in $\langle Rg \rangle$ increases (pink cloud in Fig. 2) as it enters into the diffusive domain.

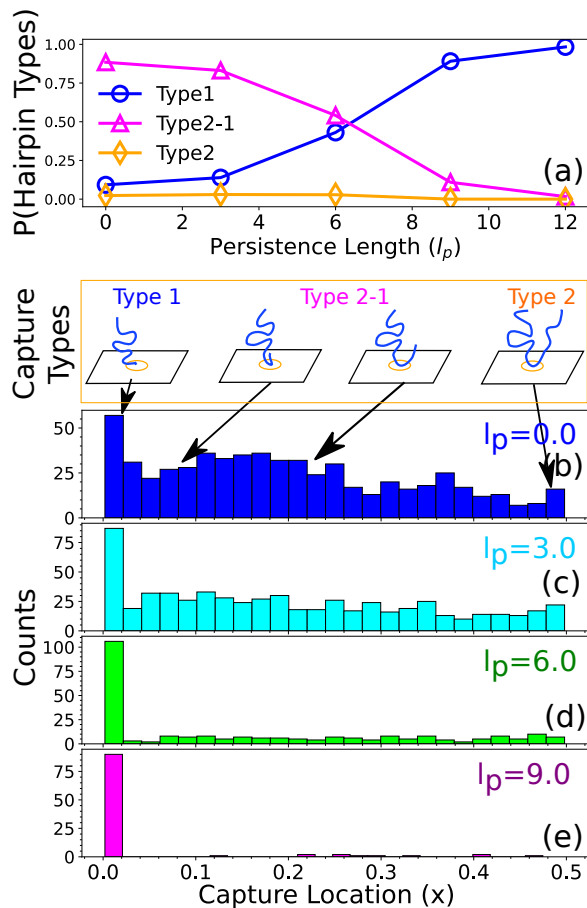


FIG. 6. (a) Hairpin capture probability for different stiffnesses of the polymer. By increasing the chain stiffness, the single file capture (Type 1 events) represented by the blue circles (\circ) increases while reducing the Type 2-1 events denoted by the magenta triangles (\triangle). The symmetric capture rate (Type 2 events) remains non-zero up to the chain persistence length $l_p = 6$ and goes to zero for stiffer chains. (b)-(e) figures show the distributions of capture locations (in reduced units) for different persistence lengths. (b) For a fully flexible polymer, capture distribution is broader, Type 2-1 event occurrence has finite translocation probability along with the Type 1 events. The capture location distributions for stiffer chains are shown in (c) $l_p = 3.0$ (d) $l_p = 6.0$ (e) $l_p = 9.0$ respectively. With the stiffening of the chain hairpin capture probability significantly reduces down improving the single file capture rate.

- **Multiple recaptures of a translocated polymer:**

It is the faster speed of translocation of a DNA in a solitary nanopore that makes the current blockade measurements noisy for sequencing purposes. To overcome this issue, multiple recaptures [18] of the same molecule can be a viable option that relies on increased statistics, hence, enhancing the accuracy of the measurement. In our simulation setup, we reverse the voltage bias as the polymer moves 20σ away from the pore after a successful translocation and study the polymer behavior depending on their stiffness during these multi-capture events. Fig. 5 demonstrates the recapture events for a polymer having the persistence length $l_p = 3.0$. Our study shows that even in the extreme narrow nanopore limit (pore diameter of 2σ), hairpin capture probability dominates over the single file translocation events for semi-flexible polymers (see the simulation movies). In addition, from Fig. 6(e) it is evident that only beyond $l_p = 6.0$, Type 1 capture probability is higher than hairpin capture (Type 2-1 and type 2) probability and $l_p = 6.0$ serves as a critical point between these two events. To understand how the chain stiffness in presence of a field gradient affects the capture process we have studied the capture location distributions shown in detail in Fig. 6(a)-(d). For a fully flexible chain ($l_p = 0$) all three types of capture occur but with the increasing stiffness single file captures become predominant. We further observe that $l_p = 3.0$ distribution - that corresponds to the persistence length of a dsDNA under most experimental conditions closely resembles the experimental capture location distribution obtained by Mihovilovic *et al.* [19].

- **Conclusion:** In this letter, we report the details of the capture and translocation of a DNA polymer as it meanders its way to the pore entrance from different equipotentials. Capture from different equipotentials affects the conformations at the pore entry as well as the translocation speed. Our studies for the first time reveal the details of multiple failed attempts and eventual success in presence of an extended E-field, quantify and differentiate accurately characteristics of translocation of both straight and folded conformations. We analyze further details of the folded coordinates in reference to the entire chain. Based on these results, we suggest how one can take advantage of it to improve the accuracy of the experimental protocol using a solitary nanopore. We also demonstrate the model is capable of reproducing all the details of an actual experiment [18] and Mihovilovic *et al.* [19]. However, as is the model, the results have validity in a much broader context and can be useful for a large community involved in biopolymer translocation.

- **Acknowledgment:** The research has been supported by grant number 1R21HG011236-01 from the National Human Genome Research Institute at the National Institute of Health. All computations were carried out using STOKES High Performance Computing Cluster at UCF. The simulation movies are generated using the Visual Molecular Dynamics package [33].

- [1] Deamer, D., Akeson, M., & Branton, D. (2016). Three decades of nanopore sequencing. *Nature Biotechnology*, 34(5), 518-524. doi:10.1038/nbt.3423
- [2] Palyulin, V. V., Ala-Nissila, T., & Metzler, R. (2014). Polymer translocation: the first two decades and the recent diversification. *Soft Matter*, 10(45), 9016-9037. doi:10.1039/c4sm01819b
- [3] Wanunu, M. (2012). Nanopores: A journey towards DNA sequencing. *Physics of Life Reviews*, 9(2), 125-158. doi:10.1016/j.plrev.2012.05.010
- [4] Keyser, U. F. (2011). Controlling molecular transport through nanopores. *Journal of The Royal Society Interface*, 8(63), 1369-1378. doi:10.1098/rsif.2011.0222
- [5] M. Muthukumar *Polymer Translocation* (CRC Press, Boca Raton, 2011).
- [6] Venkatesan, B. M., & Bashir, R. (2011). Nanopore sensors for nucleic acid analysis. *Nature Nanotechnology*, 6(10), 615-624. doi:10.1038/nnano.2011.129
- [7] Meller, A., Nivon, L., & Branton, D. (2001). Voltage-Driven DNA Translocations through a Nanopore. *Physical Review Letters*, 86(15), 3435-3438. doi:10.1103/physrevlett.86.3435
- [8] McNally, B., Singer, A., Yu, Z., Sun, Y., Weng, Z., & Meller, A. (2010). Optical Recognition of Converted DNA Nucleotides for Single-Molecule DNA Sequencing Using Nanopore Arrays. *Nano Letters*, 10(6), 2237-2244. doi:10.1021/nl1012147
- [9] Latorre-Perez, A., Villalba-Bermell, P., Pascual, J., & Vilanova, C. (2020). Assembly methods for nanopore-based metagenomic sequencing: a comparative study. *Scientific Reports*, 10(1). doi:10.1038/s41598-020-70491-3
- [10] Wang, Y., Yang, Q., & Wang, Z. (2015). The evolution of nanopore sequencing. *Frontiers in Genetics*, 5. doi:10.3389/fgene.2014.00449
- [11] Ermann, N., Hanikel, N., Wang, V., Chen, K., Weckman, N. E., & Keyser, U. F. (2018). Promoting single-file DNA translocations through nanopores using electro-osmotic flow. *The Journal of Chemical Physics*, 149(16), 163311. doi:10.1063/1.5031010
- [12] Maglia, G., Restrepo, M. R., Mikhailova, E., & Bayley, H. (2008). Enhanced translocation of single DNA molecules through hemolysin nanopores by manipulation of internal charge. *Proceedings of the National Academy of Sciences*, 105(50), 19720-19725. doi:10.1073/pnas.0808296105
- [13] Huang, S., Romero-Ruiz, M., Castell, O. K., Bayley, H., & Wallace, M. I. (2015). High-throughput optical sensing of nucleic acids in a nanopore array. *Nature Nanotechnology*, 10(11), 986-991. doi:10.1038/nnano.2015.189
- [14] Soni, G. V., & Meller, A. (2007). Progress toward Ultrafast DNA Sequencing Using Solid-State Nanopores. *Clinical Chemistry*, 53(11), 1996-2001. doi:10.1373/clinchem.2007.091231
- [15] Stoddart, D., Maglia, G., Mikhailova, E., Heron, A. J., & Bayley, H. (2009). Multiple Base-Recognition Sites in a Biological Nanopore: Two Heads are Better than One. *Angewandte Chemie International Edition*, 49(3), 556-559. doi:10.1002/anie.200905483
- [16] Liu, Q., Wu, H., Wu, L., Xie, X., Kong, J., Ye, X., & Liu, L. (2012). Voltage-Driven Translocation of DNA through a High Throughput Conical Solid-State Nanopore. *PLoS ONE*, 7(9), e46014. doi:10.1371/journal.pone.0046014
- [17] Buyukdagli, S. (2018). Facilitated polymer capture by charge inverted electroosmotic flow in voltage-driven polymer translocation. *Soft Matter*, 14(18), 3541-3549. doi:10.1039/c8sm00620b
- [18] Gershow, M., & Golovchenko, J. A. (2007). Recapturing and trapping single molecules with a solid-state nanopore. *Nature Nanotechnology*, 2(12), 775-779. doi:10.1038/nnano.2007.381
- [19] Mihovilovic, M., Hagerty, N., & Stein, D. (2013). Statistics of DNA Capture by a Solid-State Nanopore. *Physical Review Letters*, 110(2). doi:10.1103/physrevlett.110.028102
- [20] Muthukumar, M. (2010). Theory of capture rate in polymer translocation. *The Journal of Chemical Physics*, 132(19), 195101. doi:10.1063/1.3429882
- [21] Grosberg, A. Y., & Rabin, Y. (2010). DNA capture into a nanopore: Interplay of diffusion and electrohydrodynamics. *The Journal of Chemical Physics*, 133(16), 165102. doi:10.1063/1.3495481
- [22] Rowghanian, P., & Grosberg, A. Y. (2013). Electrophoretic capture of a DNA chain into a nanopore. *Physical Review E*, 87(4). doi:10.1103/physreve.87.042722
- [23] Vollmer, S. C., & de Haan, H. W. (2016). Translocation is a nonequilibrium process at all stages: Simulating the capture and translocation of a polymer by a nanopore. *The Journal of Chemical Physics*, 145(15), 154902. doi:10.1063/1.4964630
- [24] Choudhary, A., Joshi, H., Chou, H.-Y., Sarthak, K., Wilson, J., Maffeo, C., & Aksimentiev, A. (2020). High-Fidelity Capture, Threading, and Infinite-Depth Sequencing of Single DNA Molecules with a Double-Nanopore System. *ACS Nano*, 14(11), 15566-15576. doi:10.1021/acsnano.0c06191
- [25] Qiao, L., Ignacio, M., & Slater, G. W. (2019). Voltage-driven translocation: Defining a capture radius. *The Journal of Chemical Physics*, 151(24), 244902. doi:10.1063/1.5134076
- [26] Qiao, L., Ignacio, M., & Slater, G. W. (2021). An efficient kinetic Monte Carlo to study analyte capture by a nanopore: transients, boundary conditions and time-dependent fields. *Physical Chemistry Chemical Physics*, 23(2), 1489-1499. doi:10.1039/d0cp03638b
- [27] Sakaue, T. (2007). Nonequilibrium dynamics of polymer translocation and straightening. *Physical Review E*, 76(2). doi:10.1103/physreve.76.021803
- [28] Adhikari, R., & Bhattacharya, A. (2013). Driven translocation of a semi-flexible chain through a nanopore: A Brownian dynamics simulation study in two dimensions. *The Journal of Chemical Physics*, 138(20), 204909. doi:10.1063/1.4807002
- [29] Logg, A., Mardal, K.-A., & Wells, G. (Eds.). (2012). Automated Solution of Differential Equations by the Finite Element Method. *Lecture Notes in Computational Science and Engineering*. doi:10.1007/978-3-642-23099-8
- [30] Kramers, H. A., (1940) Brownian motion in a field of force and the diffusion model of chemical reactions. *Physica*, 7(4), 284-304. doi:https://doi.org/10.1016/S0031-8914(40)90098-2
- [31] Wanunu, M., Morrison, W., Rabin, Y., Grosberg,

- A. Y., & Meller, A. (2009). Electrostatic focusing of unlabelled DNA into nanoscale pores using a salt gradient. *Nature Nanotechnology*, 5(2), 160-165. doi:10.1038/nnano.2009.379
- [32] Katkar, H. H., & Muthukumar, M. (2018). Role of non-equilibrium conformations on driven polymer translocation. *The Journal of Chemical Physics*, 148(2), 024903. doi:10.1063/1.4994204
- [33] Humphrey, W., Dalke, A. and Schulten, K., "VMD: Visual Molecular Dynamics" *J. Molec. Graphics* 1996, **14**, 33-38.